Synthesis of $LiCo_{0.5}Ni_{0.5}O_2$ powders by a sol–gel method

Yang-Kook Sun,[a] In-Hwan Oh*[b] and Kwang Yul Kim[c]

[a]*Central Research Institute of Chemical Technology, Samsung Advanced Institute of Technology, 103–12 Moonji-dong, Yusong-gu, Daejeon 305–380, Korea*

[b]*Division of Chemical Engineering, Korea Institute of Science and Technology, 39–1 Hawolkok-dong, Seongbuk-ku, Seoul 136–791, Korea*

[c]*Department of Environmental Engineering, Chungbuk National University, San 48 Gaishin-dong, Heungduk-ku, Cheongju 360–763, Korea*

Layered HT (high temperature)-$LiCo_{0.5}Ni_{0.5}O_2$ powders, which are of potential interest as cathode materials for lithium secondary batteries, have been synthesized by a sol–gel method using poly(acrylic acid) (PAA) as a chelating agent. This method provided a variety of advantages of the processing conditions over the conventional solid-state reaction method. High-quality polycrystalline HT-$LiCo_{0.5}Ni_{0.5}O_2$ powders of very uniformly sized particulates with an average particle size of 0.4–2 μm could be conveniently obtained at a comparatively low calcination temperature of 600 °C and short calcination time of 1 h in air. An electrochemical study showed that the $LiCo_{0.4}Ni_{0.5}O_2$ powders had high capacity and good cycling behaviour for lithium secondary batteries.

Layered $LiCoO_2$ and $LiNiO_2$ oxides are known to be the most promising candidates for cathode materials in lithium secondary batteries with high density.[1–4] Layered lithium cobalt oxide generally shows better reversibility and higher voltage, and its preparation is easier than for layered lithium nickel oxide. Although the layered lithium nickel oxide has a high discharge capacity (>150 mA h g^{-1}),[5,6] low maximum charge voltage,[7] and a relatively lower cost, it often suffers from structural rearrangement which leads to an irreversible degradation of the electrochemical cell behaviour especially when the lithium content is lower than 0.5.[8] Therefore, the use of a solid solution system, $LiCo_{1-x}Ni_xO_2$, can be a way to optimize alternative cathode materials, since it offers a superior cycling behaviour compared to either $LiCoO_2$ or $LiNiO_2$. Recently, this system has been intensively studied for lithium secondary battery applications.[9–11]

$LiCo_{1-x}Ni_xO_2$ powders are usually prepared by the solid-state reaction method which consists of long (>24 h) and high-temperature (800–1000 °C) calcination and extended grinding of oxides, hydroxides and carbonates.[9–11] This method also provides several disadvantages in addition to the severe processing conditions: inhomogeneity, irregular morphology, large particle size with broader particle size distribution, and poor control of stoichiometry. In order to achieve a larger current capacity and reliability of the battery, it is necessary to obtain submicrometre particles of uniform morphology with narrow size distribution and homogeneity.[12,13] Several solution methods have been developed to improve the physicochemical properties of the cathode oxide materials for lithium secondary batteries.[14–16] Recently, we have reported the synthesis of ultrafine $LiCoO_2$ powders with an average particle size of 30–50 nm by a sol–gel method using PAA as a chelating agent and homogeneous $LiNiO_2$ powders by a sol–gel method using poly(vinyl butyral) (PVB).[17,18]

In this study, a synthetic process for the pure-phase $LiCo_{0.5}Ni_{0.5}O_2$ powders has been developed by a sol–gel method at relatively low temperature and short processing times using PAA as a chelating agent. The reaction mechanism of the PAA-assisted sol–gel method is discussed and the electrochemical behaviour of $LiCo_{0.5}Ni_{0.5}O_2$ is also investigated.

Experimental

$LiCo_{0.5}Ni_{0.5}O_2$ powders were prepared according to the procedure shown in Fig. 1. A stoichiometric amount of Li, Ni and Co nitrate salts with stoichiometric ratio Li : Ni : Co = 1 : 0.5 : 0.5 was dissolved in distilled water and completely mixed with an aqueous PAA solution. The molar ratio of PAA to the total metal ion content was unity. Nitric acid was slowly added to this solution with constant stirring until a pH of 1–3 was achieved. The resulting solution was then evaporated at 70–80 °C for 1 day until a transparent sol was obtained. To remove water in the sol, the transparent sol was heated at 70–80 °C while being stirred with a magnetic stirrer. As the evaporation of water proceeded, the sol turned into a viscous transparent gel. The gel precursors obtained were calcined at 500–850 °C for 1 h in air to obtain single-phase polycrystalline $LiCo_{0.5}Ni_{0.5}O_2$ powders.

The thermal decomposition behaviour of the gel precursor

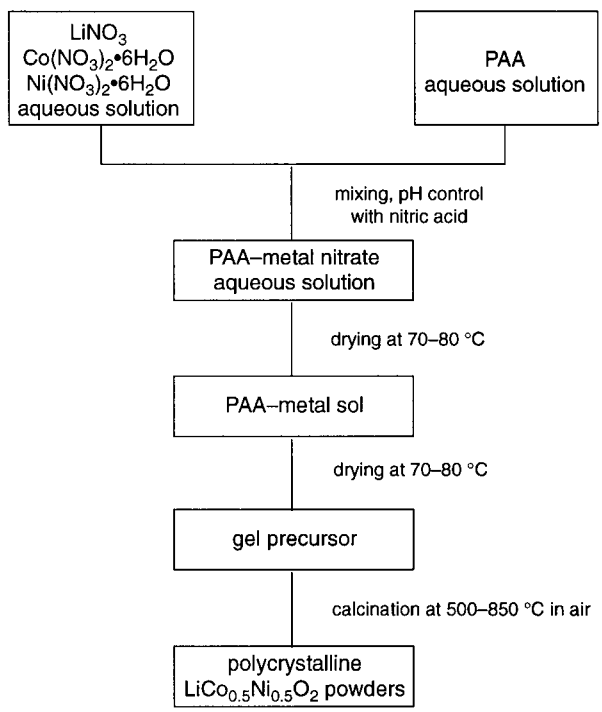

Fig. 1 Flow-chart of the preparation procedure for polycrystalline HT-$LiCo_{0.5}Ni_{0.5}O_2$ powders by a sol–gel method

was examined by thermogravimetry (TGA7, Perkin Elmer) and differential thermal analysis (DTA1700, Perkin Elmer). Powder X-ray diffraction (Rint-2000, Rigaku) using Cu-Kα radiation was used to identify the crystalline phase of the material calcined at various temperatures. The morphological changes of the particles during the calcination of the gel precursors were examined using a field emission scanning electron microscope (S-4100, Hitachi).

A three-electrode electrochemical cell was used for the galvanostatic charge–discharge experiments. The reference and counter electrodes were constructed from lithium foil (Cyprus Foote Mineral). The electrolyte used was a 1 : 1 (v/v) mixture of ethylene carbonate (EC) and propylene carbonate (PC) containing 1 M $LiClO_4$ (Mitsubishi). The Celard 2400 membrane (Hoechest Celanes) was used as the cell separator. The cathode with an active area of 6 cm^2 consisted of 0.115 g of active material (85 mass%), 0.016 g of acetylene black (12 mass%), and 0.004 g of poly(vinylidene fluoride) (PVDF; 3 mass%). This mixture was then dispersed in *N*-methylpyrollidone (NMP) and coated on the Al foil, followed by vacuum drying at 120 °C for 12 h. The cells were assembled in an argon-filled dry box. The charge–discharge cycling was galvanostatically performed at a current density of 0.25 mA cm^{-2} and a rate of 0.1 C with a cut-off voltage of 3.0–4.3 V (*vs.* $Li–Li^+$).

Results and Discussion

The transparency of the gel, which could be obtained only in the limited pH range 1–3, is a clear indication of its homogeneous composition. In a sol–gel process where PAA is used as a chelating agent, the carboxylate function CO_2^- of PAA forms a chelate with cations, resulting in a sol. The utility of PAA in the sol–gel process arises from its chemical bonding to cations in the polymer chains as represented in Fig. 2(*a*). During the sol formation process PAA acts to distribute the cations atomistically throughout the polymeric structure and prevent cation segregation and therefore precipitation. The degree of segregation largely depends on the solubility of the cations in solution as a function of pH.[19] Heating the sol to moderate temperature causes a condensation reaction between $-CO_2H$ groups *via* dehydration with the concurrent formation of water. Fig. 2(*b*) shows an example of such a reaction between $-CO_2H$ of PAA and the remaining $-CO_2H$ of chelated PAA. As most of the excess water is removed, the sol turns into a gel, and extremely high viscosity polymeric resins are formed. The gel can be either cross-linked or non-cross-linked, depending on the stoichiometry of the ratios of reactants. Since PAA has more functional groups than citric acid which is the conventional chelating agent, it should greatly aid in the formation of a cross-linked gel and this may provide more homogeneous mixing of the cations and less tendency for segregation during calcination.

Calcination of the gel in air or other gases causes breakdown of the gel. While the chemical bonding of the cations to the polymeric chains is destroyed during pyrolysis, the high viscosity of the gel causes low cation mobility, which prevents the different mixed cations from segregating. Therefore, it is assumed during the calcination that there is little segregation of the various cations that remain trapped in the char. Subsequently, the cations are oxidized to form crystallites of mixed cation oxides above 500 °C.

Fig. 3 shows thermogravimetry (TG) and differential thermal analysis (DTA) results of the gel precursors pretreated by vacuum drying at 80 °C prior to thermal analysis. It is seen that the mass loss of the gel precursors occurs in three steps, at 40–170, 170–320 and 320–370 °C, and terminates at 370 °C. The mass loss in the temperature range 40–170 °C corresponds to the removal of superficial and structural water in the gel precursors, which is accompanied by endothermic peaks at

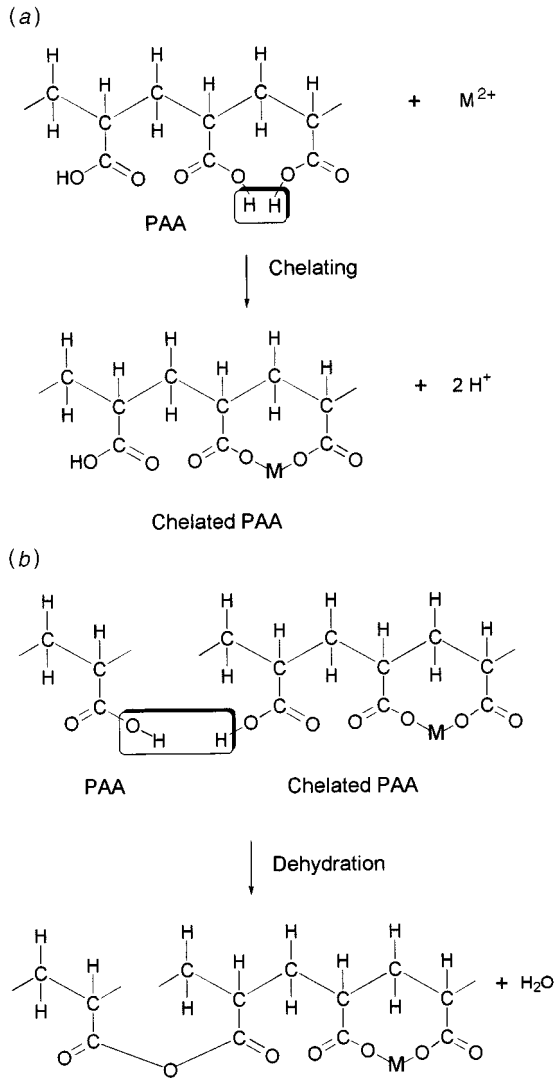

Fig. 2 Reaction mechanism of the PAA-assisted sol–gel process: (*a*) chelating reaction and (*b*) dehydration

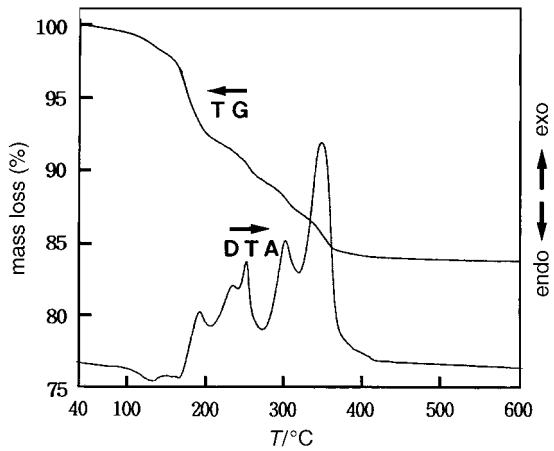

Fig. 3 Thermogravimetry and differential thermal analysis of the gel precursors pretreated by vacuum drying at 80 °C prior to thermal analysis in an air flow rate of 40 cm^3 min^{-1} and a heating rate of 5 °C min^{-1}

133 and 167 °C in the DTA curve. The mass loss in the temperature range 170–320 °C is associated with the combustion of inorganic and organic constituents in the gel precursors such as nitrates and PAA, related to the exothermic peaks at 192, 234, 252 and 300 °C in the DTA curve. The exothermic peak at 234 °C appeared to be due to the decomposition of nitrate. Similar behaviour has been previously reported where nitrate decomposition in PAA–nitrate gels and citrate–nitrate gels took place at 229 °C and $\gtrsim$200 °C, respectively.[17,20] The exothermic peaks at 192, 252, and 300 °C could be considered as a result of the decomposition of PAA, since the gel precursors were self-burning once ignited. This phenomenon is supported by the observation that the gel precursors turned into fluffy dark brown powders after calcination at 300 °C. This result has been also observed when $La_{1-x}Sr_xMnO_3$ gel precursors using PAA as a chelating agent were decomposed, although the order of the exothermic peak magnitude was reversed.[21] This behaviour may be due to differences in the strength of interaction between PAA and various metal ions. The mass loss in the temperature range 320–370 °C indicates the combustion of remaining organic constituents in the gel precursors, accompanied by the largest exothermic peak at 350 °C in the DTA curve.

The X-ray diffraction (XRD) patterns for the gel-derived materials calcined at various temperatures for 1 h in air are shown in Fig. 4. For the material calcined at 500 °C, impurity peaks as well as the $LiCo_{0.5}Ni_{0.5}O_2$ phase were observed. When calcination was carried out at 600 °C, a single phase of high-temperature (HT) $LiCo_{0.5}Ni_{0.5}O_2$ formed; it took $<$1 h to achieve full crystallinity. Generally, the higher the calcination temperature, the sharper and higher the diffraction peaks became, indicating improved crystallinity of $LiCo_{0.5}Ni_{0.5}O_2$. These results strongly suggest that the sol–gel preparation method requires much lower calcination temperatures and shorter calcination times than the solid-state reaction where the calcination temperature is usually 800–1000 °C and calcination time is $>$24 h. The results clearly indicate that the use of PAA greatly suppresses the formation of precipitates leading to heterogeneity, since the cross-linked gel may provide more homogeneous mixing of the cations and less tendency for segregation during calcination. Therefore, the finely mixed state of the calcined materials in the homogeneous composition makes it possible to form a single-phase HT-$LiCo_{0.5}Ni_{0.5}O_2$

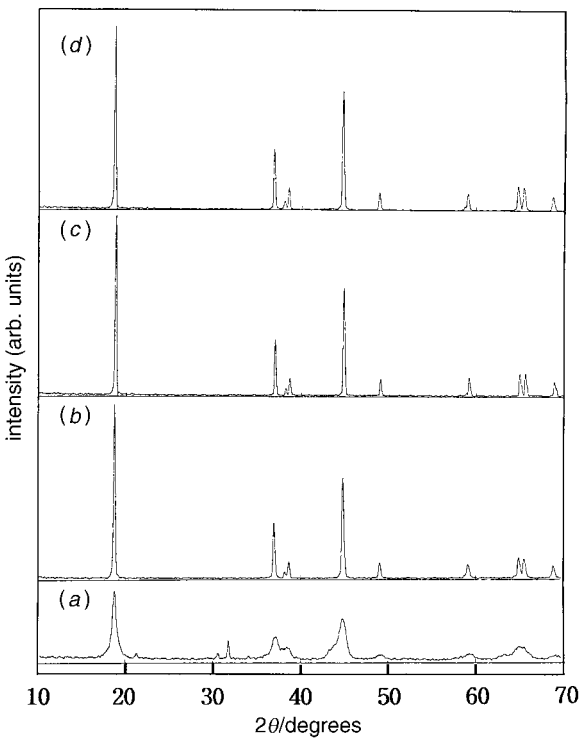

Fig. 4 X-Ray diffraction patterns of gel-derived materials calcined at various temperatures for 1 h in air: (*a*) 500 °C, (*b*) 600 °C, (*c*) 750 °C and (*d*) 850 °C

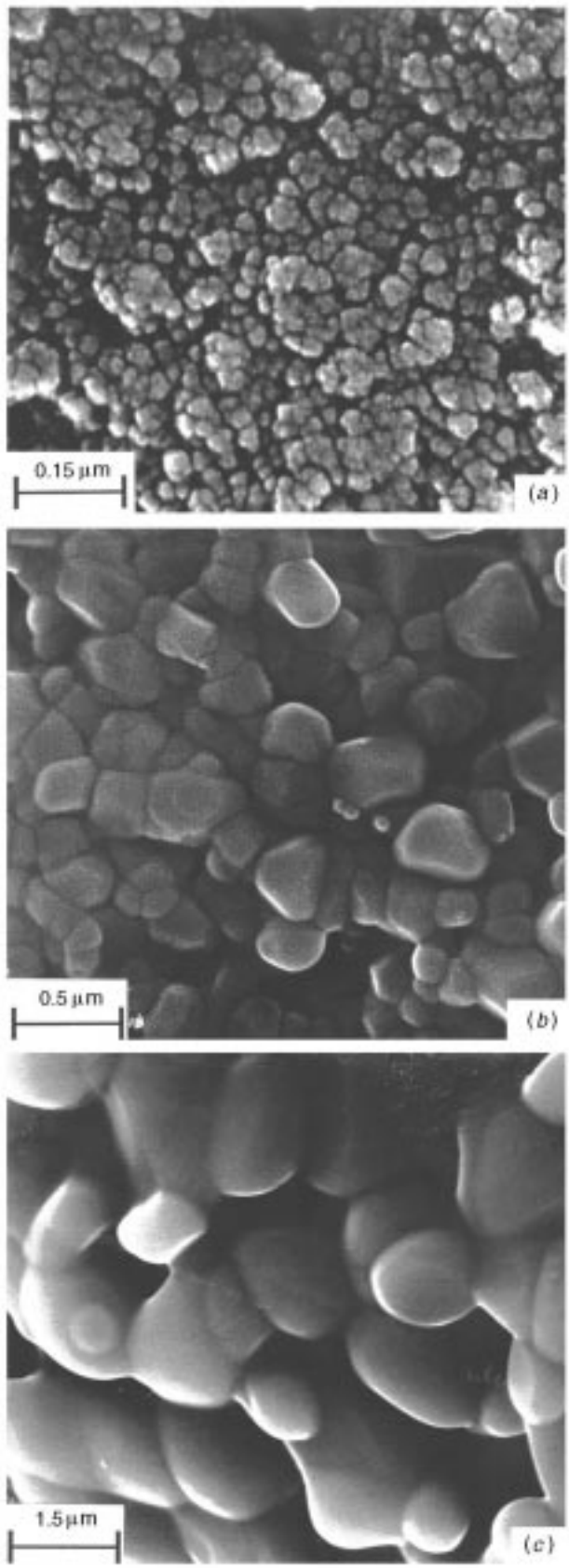

Fig. 5 Scanning electron micrographs of the powders calcined at various temperatures for 1 h in air: (*a*) 500 °C, (*b*) 600 °C and (*c*) 750 °C

under mild conditions. This may be ascribed to the fact that the materials derived from the gel precursors are of atomic scale, are homogeneously mixed, and thus have high sinterability. Similar results have been reported for $LiCoO_2$ powders synthesized through the sol–gel method using PAA as a chelating agent for LT (low temperature)-$LiCoO_2$ and HT-$LiCoO_2$ powders at 400 and 550 °C for 1 h, respectively.[17]

Fig. 5 shows scanning electron microscope (SEM) images for the powders calcined at various temperatures for 1 h in air. The presence of loosely agglomerated spherical particles whose average grain size was 40 nm was observed from the powders calcined at 500 °C. As the calcination temperature increases, growth kinetics are favoured and thus the agglomerated spherical particles become larger. For the materials calcined at 600 °C the particle size of the particulates ranges from 0.24 to 0.5 μm (coverage is *ca.* 0.4 μm). When the gel precursors were heated at 750 °C, the particle size of the particulates increased to 2 μm with a fairly narrow particle size distribution. This was confirmed by sharper and higher diffraction peaks in the XRD patterns. From the above results, it is concluded that $LiCo_{0.5}Ni_{0.5}O_2$ powders with a wide variety of physicochemical properties such as particle size and microcrystallite morphologies can be synthesized by simply varying the pyrolysis processing parameters such as calcination temperature and time.

Fig. 6(*a*) shows the charge–discharge characteristics and cyclability of Li/$LiCo_{0.5}Ni_{0.5}O_2$ (calcined at 750 °C) cells for the first ten cycles at a constant charge–discharge current density of 0.25 mA cm^{-2} and a rate of 0.1 C between 3.0 and 4.2 V. Fig. 6(*b*)–(*d*) shows the first, fifth and tenth cycle, respectively. The $LiCo_{0.5}Ni_{0.5}O_2$ powders show very good reversibility of the Li ion intercalation–deintercalation process. Also, the polarization, which is half of the difference in voltage between the charge and discharge curves, is very low (0.0121, 0.0191 and 0.0191 V at 82 mA h g^{-1} for the first, fifth and tenth cycle, respectively) compared to the value reported by Saadoune and Delmas[11] (*ca.* 0.05 V at $x=0.7$), although the current density in our study, 0.25 mA cm^{-2}, is higher than that used in ref. 11 (70 μA cm^{-2}). Note that the specific capacity of 82 mA h g^{-1} in Fig. 6(*b*)–(*d*) corresponds to the composition of $x=0.7$ in the sixth figure of Fig. 7 of ref. 11. It is also seen from Fig. 6(*a*) that polarization does not increase with cycling.

The discharge capacity *vs.* cycle number is shown in Fig. 7. The Li/$LiCo_{0.5}Ni_{0.5}O_2$ cell initially delivers 165 mA h g^{-1}, which to our knowledge is the highest value obtained and is even better than the result (138 mA h g^{-1}) of Ohzuku *et al.*,[22] although the test conditions were different. The capacity slowly decreases with cycling and was 130 mA h g^{-1} by the tenth cycle. While the capacity shows a decrease upon cycling, the polarization remains almost unchanged. This means that the main cause of capacity fading is not due to the cathode but probably arises from oxidation of the electrolyte. Ohzuku *et al.* reported that the rechargeable capacity (cyclability) of $LiCo_{0.5}Ni_{0.5}O_2$ is highly dependent upon the stability of the electrolyte.[22] Therefore, it is necessary to select a stable solvent and solute against oxidation for the Li/$LiCo_{0.5}Ni_{0.5}O_2$ cell to improve cyclability.

We believe that the $LiCo_{0.5}Ni_{0.5}O_2$ powders synthesized in this study will be of great impact in improving the electrochemi-

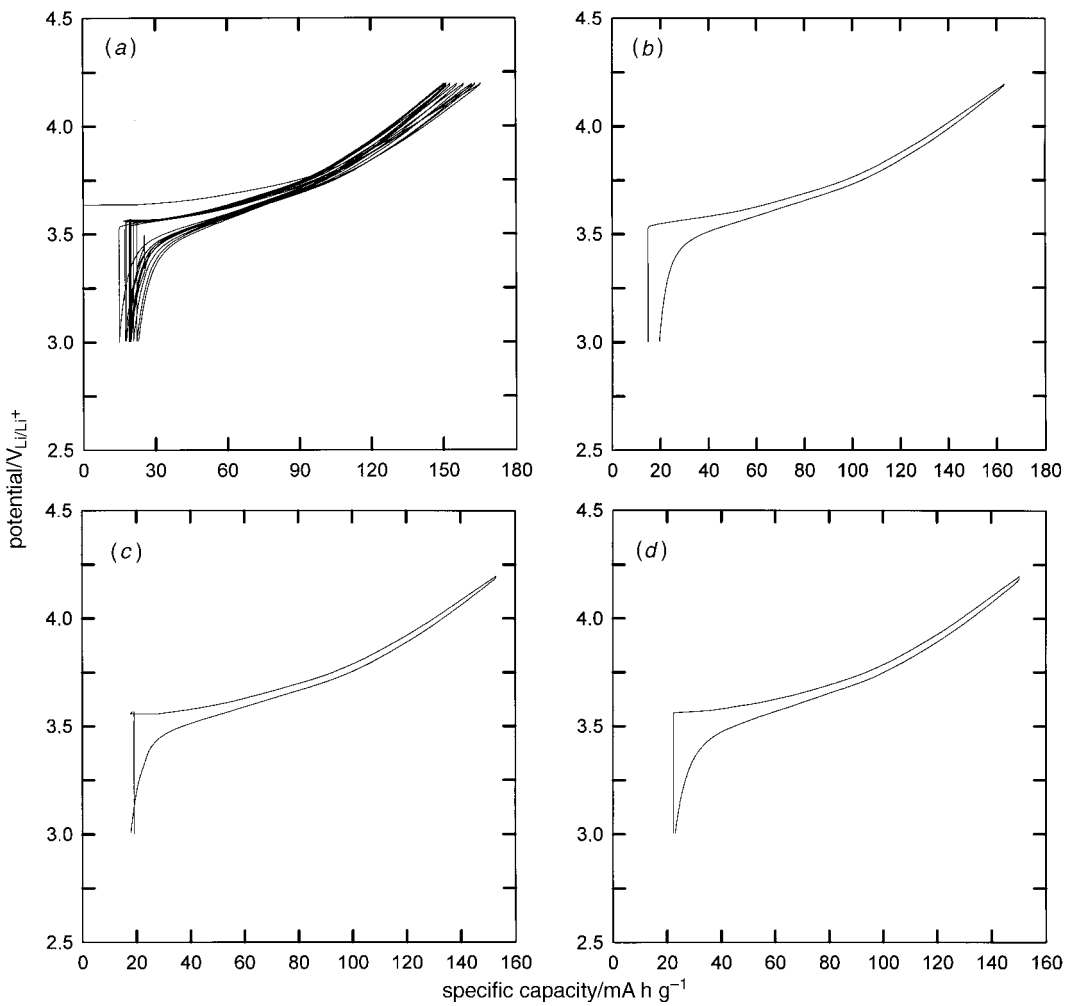

Fig. 6 Charge–discharge curves over the potential ranges 3.0–4.2 V at a current density of 0.25 mA cm^{-2} for the cells of Li/$LiClO_4$–EC–PC/$LiCo_{0.5}Ni_{0.5}O_2$: (*a*) 10 cycles, (*b*) 1st cycle, (*c*) 5th cycle, and (*d*) 10th cycle

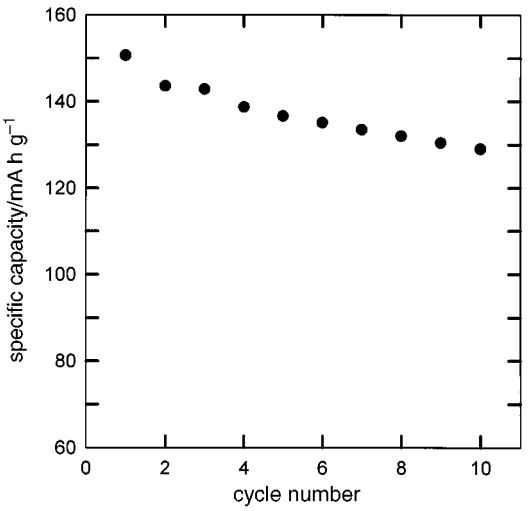

Fig. 7 Discharge capacities *vs.* cycle number

cal, magnetic, and mechanical properties of materials in practical applications as a cathode active material for lithium secondary batteries. In the future, a more detailed electrochemical study will be carried out in an attempt to improve cyclability.

Conclusions

$LiCo_{0.5}Ni_{0.5}O_2$ powders have been synthesized by the sol–gel method using an aqueous solution of metal nitrates containing PAA as the chelating agent. Single-phase HT-$LiCo_{0.5}Ni_{0.5}O_2$ powders were obtained at 600 °C after 1 h in air; the calcination temperature and time were much lower than in the conventional solid-state reaction method. The crystalline products calcined at 600 and 750 °C contained fairly narrow and uniform spherical particulates with average particle sizes of 0.4 and 2 μm, respectively. Electrochemical studies showed that the PAA-assisted $LiCo_{0.5}Ni_{0.5}O_2$ powders had a high initial performance of 165 mA h g^{-1} and also a good cycling performance.

References

1 K. Mizushima, P. C. Jones, P. J. Wiseman and J. B. Goodenough, *Mater. Res. Bull.*, 1980, **15**, 783.
2 L. Plomp, E. F. Sitters, C. Vessies and F. C. Eckes, *J. Electrochem. Soc.*, 1991, **138**, 629.
3 J. B. Veldhuis, F. C. Eckes and L. Plomp, *J. Electrochem. Soc.*, 1992, **139**, L6.
4 T. Miyashita, H. Noguchi, K. Yamato and M. Yoshio, *J. Ceram. Soc. Jpn.*, 1994, **102**, 258.
5 T. Ohzuku, A. Ueda and M. Nagayama, *J. Electrochem. Soc.*, 1991, **140**, 1862
6 W. Li, J. N. Reimers and J. R. Dahn, *Solid State Ionics*, 1993, **67**, 123.
7 R. V. Moshtev, P. Zlatilova, V. Manev and A. Sato, *J. Power Sources*, 1995, **54**, 329.
8 W. Li, J. N. Reimers and J. R. Dahn, *Phys. Rev.*, 1992, **46**, 3236.
9 C. Delmas and I. Saadoune, *Solid State Ionics*, 1992, **53–56**, 370.
10 E. Zhecheva and R. Stoyanova, *Solid State Ionics*, 1993, **66**, 143.
11 I. Saadoune and C. Delmas, *J. Mater. Chem.*, 1996, **6**, 193.
12 J. N. Reimers and J. R. Dahn, *J. Electrochem. Soc.*, 1992, **139**, 2091.
13 N. Miyamoto and I. Tanabe, *Denki Kagaku*, 1990, **58**, 663.
14 P. Barboux, J. M. Tarascon and F. K. Shokoohi, *J. Solid State Chem.*, 1991, **94**, 185.
15 T. Tsumura, A. Shimizu and M. Inagaki, *J. Mater. Chem.*, 1993, **3**, 995.
16 S. Prabaharan, M. S. Michael, T. P. Kumar, A. Mani, K. Athinarayanaswamy and R. Gangadharan, *J. Mater. Chem.*, 1995, **5**, 1035.
17 Y-K. Sun, I-H. Oh and S-A. Hong, *J. Mater. Sci.*, 1996, **31**, 3617.
18 Y-K. Sun, I-H. Oh and S-A. Hong, *J. Mater. Sci. Lett.*, 1997, **16**, 30.
19 P. A. Lessing, *Ceram. Bull.*, 1989, **68**, 1002.
20 M. S. G. Baythoun and F. R. Sale, *J. Mater. Sci.*, 1982, **17**, 2757.
21 H. Taguchi, D. Matsuda and M. Nagao, *J. Am. Ceram. Soc.*, 1992, **75**, 201.
22 T. Ohzuku, A. Ueda, M. Nagayama, Y. Iwakoshi and H. Komori, *Electrochim. Acta*, 1993, **38**, 1159.

Paper 6/07550I; *Received* 5th *November*, 1996